Journal of Cell Communication and Signaling (2023) 17:263–274
https://doi.org/10.1007/s12079-023-00740-3

RESEARCH ARTICLE

BMP-1-induced GBA1 nuclear accumulation provokes CCN2 mRNA expression via importin-β-mediated nucleocytoplasmic pathway

Koichiro Muromachi[1] · Rei Nakano[2,3] · Junko Fujita-Yoshigaki[4] · Hiroshi Sugiya [3,5] · Nobuyuki Tani-Ishii[1]

Received: 9 January 2023 / Accepted: 13 March 2023 / Published online: 27 March 2023

Abstract

Bone morphogenetic protein (BMP)-1 is expressed by odontoblasts in the dentin-pulp complex. Although the functional effects of BMP-1 on the maturation of various preforms of proteins and enzymes involved in initiating mineralization have been widely observed, how BMP-1 affects cellular molecules remains unknown. We performed a comprehensive analysis of BMP-1-altered glycome profiles and subsequent assays to identify the target glycoproteins in human dental pulp cells (hDPCs) by a glycomic approach. In the presence of BMP-1, a lectin microarray analysis and lectin-probed blotting showed that α2,6-sialylation was significantly attenuated in insoluble fractions from hDPCs. Six proteins were identified by a mass spectrometry analysis of α2,6-sialylated glycoproteins purified using a lectin column. Among them, glucosylceramidase (GBA1) was found to accumulate in the nuclei of hDPCs in the presence of BMP-1. Moreover, BMP-1-induced cellular communication network factor (CCN) 2 expression, which is well known as the osteogenesis/chondrogenesis marker, was significantly suppressed in the cells transfected with GBA1 siRNA. Furthermore, importazole, a potent inhibitor of importin-β-mediated nuclear import significantly suppressed BMP-1-induced GBA1 nuclear accumulation and BMP-1-induced CCN2 mRNA expression, respectively. Thus, BMP-1 facilitates the accumulation of GBA1 in the nucleus through the reduction of α2,6-sialic acid, which potentially contributes to the transcriptional regulation of the CCN2 gene via importin-β-mediated nuclear import pathway in hDPCs. Our results offer new insights into the role of the BMP-1-GBA1-CCN2 axis in the development, tissue remodeling, and pathology of dental/craniofacial diseases.

✉ Koichiro Muromachi
muromachi@kdu.ac.jp

[1] Department of Endodontics, Graduate School of Dentistry, Kanagawa Dental University, Yokosuka, Kanagawa 238-8580, Japan

[2] Laboratory for Mucosal Immunity, Center for Integrative Medical Sciences, RIKEN Yokohama Institute, Yokohama, Kanagawa 230-0045, Japan

[3] Laboratory of Veterinary Radiology, Department of Veterinary Medicine, College of Bioresource Sciences, Nihon University, Fujisawa, Kanagawa 252-0880, Japan

[4] Department of Physiology, Nihon University School of Dentistry at Matsudo, Matsudo, Chiba 271-8587, Japan

[5] Japan Animal Specialty Medical Institute (JASMINE), Yokohama, Kanagawa 224-0001, Japan

Graphical abstract

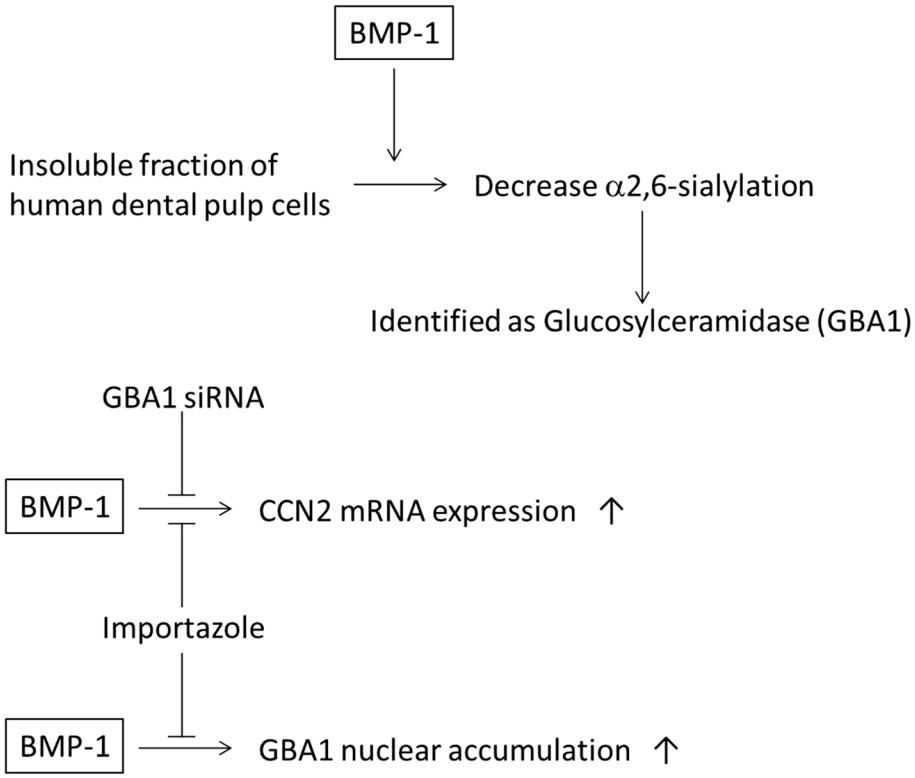

Keywords Glycomics · Lectin microarray · LC-MS · MS analysis · Sialylation · Glycosphingolipid

Abbreviations

BMP-1	Bone morphogenetic protein-1
hDPCs	Human dental pulp cells
α2,6-sia	α2,6-Linked sialic acid
GBA1	Glucosylceramidase
mTLD	Mammalian tolloid protein
DMP-1	Dentin matrix protein-1
DSPP	Dentin sialophosphoprotein
CCN2	Cellular communication network factor 2
rhBMP-1	Recombinant human BMP-1
SNA	*Sambucus nigra* agglutinin
SSA	*Sambucus sieboldiana* agglutinin
TJA-I	*Trichosanthes japonica* agglutinin-I
SDS-PAGE	Sodium dodecyl sulfate-polyacrylamide gel electrophoresis
CBB	Coomassie brilliant blue
LAMP1	Lysosome associated membrane protein 1
DAPI	4′,6-Diamidino-2-phenylindole
GlcCer	Glucosylceramide
GBA2	Non-lysosomal β-glucosylceramidase
GBA3	Cytosolic β-glucosidase
KLrP	Klotho-related protein
O-GlcNAc	*O*-Linked *N*-acetylglucosamine
GAPDH	Glyceraldehyde-3-phosphate dehydrogenase

Introduction

Bone morphogenetic protein (BMP)-1 was isolated as an ectopic ossification factor from bone extracts (Urist et al. 1973; Wozney et al. 1988). BMP-1 and its isoform mammalian tolloid protein (mTLD) are encoded by alternatively spliced transcripts of the *BMP1* gene (Takahara et al. 1994). A recent study found that patients with the osteogenesis imperfecta phenotype show mutations in the *BMP-1* gene. This report also mentioned that some of the patients had tooth fragility and tooth hypoplasia, suggesting that BMP-1 is involved in tooth development (Syx et al. 2015). Previous studies have suggested the involvement of BMP-1 in dentin formation through processing type I-III procollagen (Kessler et al. 1996; Li et al. 1996) and dentin-specific proteins, such as dentin matrix protein-1 (DMP-1) (Steiglitz et al. 2004) and dentin sialophosphoprotein (DSPP) (von Marschall and Fisher 2010; Tsuchiya et al. 2011). Our previous immunohistochemical study revealed that dental caries provoked the

expression of BMP-1 in odontoblast-like cells and reparative dentin in the human dentin-pulp complex (Muromachi et al. 2015). Proteomic analysis revealed that the expression of BMP-1 is specific to odontoblasts but not in the central region of the pulp (Abbey et al. 2018). Recently, Wang et al. reported the impairment of dentin maturation and root formation in BMP-1/TLL1 double-knockout mice (Wang et al. 2017). Taken together, these findings suggest that BMP-1 has a critical role in tooth formation as a catalytic enzyme for collagenous and non-collagenous proteins of dentin. However, while the involvement of BMP-1 in the biosynthesis of the dentin components has been widely observed, whether BMP-1 interacts with cellular molecules remains unclear. We previously showed that the expression of the osteogenesis marker cellular communication network factor (CCN) 2 was increased by the dynamin-dependent endocytosis of BMP-1 in human dental pulp cells (hDPCs) (Muromachi et al. 2015). It is thus tempting to speculate that BMP-1 may act as a signaling molecule.

Protein glycosylation is one of the most common post-translational modifications. The glycan profile varies among cell types and degrees of cellular differentiation (Varki 1993). The degree of cellular differentiation alters the glycan structure in membrane glycoproteins, suggesting that specific glycosylation of certain proteins is an essential component of cellular physiology. One example of changes in cell surface glycan structures is the induction of pluripotency (Tateno et al. 2011).

In the present study, we conducted a comprehensive analysis to identify a targeting molecule of BMP-1 in hDPCs by a glycomic approach.

Materials and methods

Ethics statement

This study was approved by the ethics committee of Kanagawa Dental University (No. 277). The patients gave their informed consent before providing samples.

Cell culture

hDPCs were collected from three intact third molars under aseptic conditions as previously described (Muromachi et al. 2015). For the experiments, the cells from passages 3–5 were used.

Preparation of insoluble fractions

hDPCs were seeded at 2×10^5 cells/ml α-MEM containing 10% fetal bovine serum (FBS) in 100 mm tissue culture dishes. Semi-confluent cells were starved in a medium containing 1% FBS for 24 h and then stimulated in serum-free medium with 500 ng/ml recombinant human BMP-1 (rhBMP-1) (R&D Systems, Minneapolis, MN, USA) for 60 min. Insoluble and soluble fractions were prepared with a Mem-PER Eukaryotic Membrane Protein Extraction Reagent Kit (Pierce Chemical, Rockford, IL, USA) according to the manufacturer's protocols. After phase partition, the insoluble fraction contains membrane and membrane-associated proteins, and the soluble fraction contains soluble cytoplasmic proteins. The method of Bradford was used to adjust the protein concentrations (Bradford 1976).

The lectin microarray analysis

The analysis of BMP-1-altered glycosylation profiles in insoluble fractions from hDPCs was performed by GlycoTechnica, Ltd. (Yokohama, Japan). Protein samples were labeled with Cy3 mono-reactive dye at room temperature for 1 h. The unbounded Cy3 dye was removed using desalting columns. We first measured the lectin binding signals of each concentration of Cy3-labeled protein samples (31.25, 62.5, 125, 250, 500, 1000, 2000 ng/ml) and identified the optimal concentration as 250 ng/ml. After diluting to 250 ng/ml in probing solution, aliquots of the dye-labeled sample (100 µl/well) were applied onto a LecChip® and incubated at 20 °C for 18 h. The fluorescence intensities on each lectin-coated spot were monitored using an evanescent-field fluorescence scanner GlycoStation Reader 1200 (GlycoTechnica).

Lectin-probed blotting

Protein samples were boiled at 95 °C for 5 min in SDS sample buffer. Subsequently, equal amounts of samples (10 µg) were resolved by sodium dodecyl sulfate-polyacrylamide gel electrophoresis (SDS-PAGE) in a 7.5% polyacrylamide gel and transferred to nitrocellulose membranes overnight (12 V). The membranes were blocked at room temperature for 50 min in RIPA buffer (Sigma-Aldrich, Dorset, UK) and then probed for 120 min with HRP-conjugated *Sambucus nigra* agglutinin (SNA) (SNA-I, H-6802-1, diluted 1:2000; EY Laboratories, San Mateo, CA, USA). After incubation, the blots were washed three times with RIPA buffer. The signals were detected using an ECL prime (GE, Piscataway, NJ, USA). As a loading control, the same samples were analyzed by Western blotting with a primary antibody of rabbit anti-caveolin-1 (3267 S, diluted 1:1000; Cell Signaling Technology, Danvers, MA, USA) and secondary antibody of anti-rabbit IgG HRP-linked (7074, diluted 1:2000; Cell Signaling Technology). The gel images were scanned on a LAS-3000 (Fuji, Tokyo, Japan).

Enrichment of glycoprotein

SNA-binding glycoproteins were enriched using AffiSpin® SNA kit (GALAB Technologies, Hamburg, Germany). In brief, insoluble fractions were suspended in adsorption buffer and applied to an AffiSpin® lectin column. After washing two times with adsorption buffer, SNA-binding glycoproteins were eluted two times from the affinity column with elution buffer B (sialyl-lactose). After elution, the column was washed two times with adsorption buffer. Each collected elution fraction and wash fraction was confirmed by SDS-PAGE and CBB staining (CBB stain One Super; Nacalai Tesque, Kyoto, Japan).

Mass spectrometry

The eluate was desalted and concentrated by diafiltration using an Amicon Ultra centrifugal filter device (Ultracel-30, cut-off: 30 kDa; Millipore, Billerica, MA, USA). The concentrate and filtrate were separated by SDS-PAGE and stained with CBB. CBB-stained bands of the enriched samples excised from an SDS-PAGE gel were analyzed by LC-MS/MS. LC-MS/MS was performed by Shimadzu Techno-Research (Kyoto, Japan). Briefly, gel samples were reduced and alkylated by DTT/iodoacetamide. Each sample was digested with trypsin at 37 °C overnight. For reaction monitoring an Easy-nLC 1000™ (Thermo Fisher Scientific, Rockford, IL, USA) was used. The HPLC was coupled to a Q-Exactive Plus mass spectrometer (Thermo Fisher Scientific) and ionization was carried out with ESI positive mode. Solvent A contained 0.1% formic acid and solvent B contained 100% acetonitrile with 0.1% formic acid. The following gradient (vol% solvent B/time) was used: 0–40%/0-10 min, 40–100%/10-12 min, 100–100%/12-20 min with a flow rate of 300 nL/min. The proteins were identified by searching the SwissProt database using MASCOT (Matrix Science Inc., UK) and the Proteome Discoverer 1.4 software (Thermo Fisher Scientific) with the following parameters: A peptide mass tolerance of ± 10 ppm and a fragment mass tolerance of ± 0.02 Da were used.

Western blotting

Soluble fractions (2 μg) and insoluble fractions (10 μg) were separated by SDS-PAGE and transferred to nitrocellulose membranes overnight (12 V). Non-specific binding was blocked by Block Ace (DS Pharma Biomedical, Osaka, Japan). The membranes were probed with the primary antibody specific for GBA1 (rabbit anti-GBA, ab125065, diluted 1:1000; Abcam, Cambridge, UK) for 120 min. The blots were washed 3 times with 10% Block Ace containing 0.05% Tween-20 and subsequently probed with the secondary antibody anti-rabbit IgG HRP-linked (7074, diluted 1:2000; Cell Signaling Technology) for 60 min. Detection of immunoreactivity was performed using ECL prime.

Immunofluorescence

hDPCs seeded at a density of 7×10^4 cells/ml medium in a chamber slide (Matsunami, Tokyo, Japan) were stimulated with rhBMP-1 (500 ng/ml) for 5, 15, 30, 60, and 180 min. After fixation using 4% paraformaldehyde for 15 min or ice-cold methanol (−20 °C) for 10 min, the cells were permeabilized by phosphate-buffered saline (PBS) containing 0.1% Triton X-100 for 15 min. Non-specific reactions were blocked by Block Ace for 30 min. The cells were then incubated with rabbit anti-GBA1 antibody (1:100) in a moist chamber overnight at 4 °C. The slides were washed 3 times with PBS containing 0.2% Tween-20 (PBST) and then probed for 60 min with Alexa Fluor 594-conjugated F(ab′)2 fragments of goat anti-rabbit IgG (H + L) (A11072, diluted 1:1000; Life Technologies, Carlsbad, CA, USA). The cells were also incubated with only a secondary antibody as a control for the nonspecific binding of the antibody. After washing with PBST, the slides were incubated with Alexa Fluor 488 phalloidin (for filamentous actin staining; Life Technologies) for 20 min in the dark. The samples were then mounted using ProLong gold anti-fade reagent with 4′,6-diamidino-2-phenylindole (DAPI, for nuclear staining; Life Technologies). For lysosome staining, mouse anti-LAMP1 (15,665, diluted 1:100; Cell Signaling Technology) as a primary antibody and goat anti-mouse IgG H&L (Alexa Fluor 488) preadsorbed (ab150117, diluted 1:1000; Abcam) as a secondary antibody were used. The images were acquired using an LSM 510 META confocal microscope (Carl Zeiss, Oberkochen, Germany). GBA1 signals were observed in three randomly chosen sites per three different experiments. The fluorescence intensity of each nucleus showing GBA1 signals was measured. The mean fluorescence intensity was calculated by dividing the total fluorescence intensity per nucleus by the number of cells.

siRNA transfection

hDPCs were seeded at 1×10^5 cells/35 mm dish or 5×10^5 cells/90 mm dish in α-MEM containing 10% FBS. These cells were transfected using Opti-MEM containing 5 μL/mL Lipofectamine 2000 and 200 nM GBA1 siRNA (NM_000157 and NM_001005741, Sigma-Aldrich) or scramble siRNA (SIC001, Sigma-Aldrich) for 24 h. After incubation, the cells were collected for subsequent analyses.

Real-time RT-PCR

Total RNA was extracted from hDPCs with TRIzol reagent. The first-strand cDNA synthesis was carried out with 500

ng of total RNA using PrimeScript RT Master Mix. Real-time RT-PCR was performed with 2 μL of the first-strand cDNA in 25 μL (total reaction volume) with SYBR Premix Ex Taq II and primers specific for CCN2 and glyceraldehyde-3-phosphate dehydrogenase (GAPDH, a house keeping gene used as a control). Real-time RT-PCR of no-template controls was performed with 2 μL of RNase- and DNA-free water. Additionally, real-time PCR of no-reverse transcription control was performed with 2 μL of each RNA sample. PCR was conducted using Thermal Cycler Dice Real Time System II using the following protocol: 1 cycle of denaturing at 95 °C for 30 s, 40 cycles of denaturing at 95 °C for 5 s and annealing/extension at 60 °C for 30 s. The results were analyzed by the second derivative maximum method and the comparative cycle threshold (ΔΔ Ct) method using real-time RT-PCR analysis software. The amplification of GAPDH from the same amount of cDNA was used as endogenous control, while cDNA amplification from hDPCs at time 0 was used as a calibration standard.

Statistical analyses

The results are presented as the means ± standard error (SE) from three different experiments. Statistical analyses were performed using the Excel Statistics, 2015 (SSRI, Tokyo, Japan) software program. The data were analyzed by one-way analysis of variance. Group means were compared by Tukey's multiple comparison test.

Results

Identification of BMP-1-targeted glycoprotein using lectin microarray and mass spectrometric analysis

First, to investigate whether or not BMP-1 affects cellular molecules, we focused on the glycome shift and conducted a lectin microarray. In the presence of rhBMP-1, three lectins showed a significant reduction of signals: SNA, *Sambucus sieboldiana* agglutinin (SSA), and *Trichosanthes japonica* agglutinin-I (TJA-I) (Fig. 1A). These lectins commonly recognize α2,6-linked sialic acid (α2,6-sia). The BMP-1/Control ratio showed 0.49-, 0.52-, and 0.55-fold decreases in signal intensity. *P*-values of signal intensities of each lectin between the absence or presence of BMP-1 showed 0.00024, 0.00094, and 0.00080, respectively. To further validate the lectin microarray results, we performed SDS-PAGE and lectin-probed blotting with the HRP-conjugated lectin SNA. The SNA detected 2 major bands at apparent molecular weights between 50 and 75 kDa (Fig. 1B). In contrast to the controls, the administration of rhBMP-1 consistently attenuated the α2,6-sialylation of insoluble fractions. Given the above, we selected α2,6-sialylation as a putative glycan change that could be targeted by BMP-1 in hDPCs. Next, since the α2,6-sia modification of proteins was significantly reduced by BMP-1, we sought to identify SNA-binding glycoproteins in the insoluble fractions of hDPCs. As an initial step, α2,6-sialylated glycoproteins were enriched using an SNA lectin column and eluted by the competing oligosaccharide sialyl-lactose. Each fraction was resolved by SDS-PAGE and confirmed by SNA lectin blotting. Purified α2,6-sialylated glycoproteins were identified as 2 bands within the eluted fractions at apparent molecular weights between 50 and 75 kDa (Fig. 1C). Subsequently, enriched samples were concentrated by diafiltration. The concentrate and filtrate were separated by SDS-PAGE and stained with coomassie brilliant blue (CBB). Visual inspection of the gel revealed that 3 bands were distributed between 50 and 75 kDa in the concentrate lane (Fig. 1D). Marked bands 1 to 3 were excised from the gel and analyzed by liquid chromatography with tandem mass spectrometry (LC-MS/MS). The identified proteins are shown in Table 1. We identified the SNA-binding glycoproteins as serotransferrin, serpin A12, Glucosylceramidase (GBA1), keratin type II cytoskeletal 2 epidermal, InaD-like protein, and pyruvate kinase.

BMP-1 facilitates the accumulation of GBA1 in the nuclei

Among the 6 identified glycoproteins, we first detected the changes in GBA1 at an apparent molecular weight of 60 kDa in the insoluble fraction of hDPCs by Western blotting

Table 1 Identification of α2,6-sialylated glycoproteins in hDPCs. CBB-stained bands 1 to 3 of the enriched samples excised from an SDS-PAGE gel (Conc. lane) were analyzed by LC-MS/MS.

	Accession No.	Protein assigned	Mascot score	Sequence coverage	# Peptides
Band 1	P02787	Serotransferrin	220.35	8.74	6
	Q8IW75	Serpin A12	30.35	1.21	1
Band 2	P04062	Glucosylceramidase	118.63	6.53	3
	P35908	Keratin, type II cytoskeletal 2 epidermal	33.83	2.50	1
Band 3	Q8NI35	InaD-like protein	70.77	0.33	1
	P14618	Pyruvate kinase PKM	35.25	2.07	1

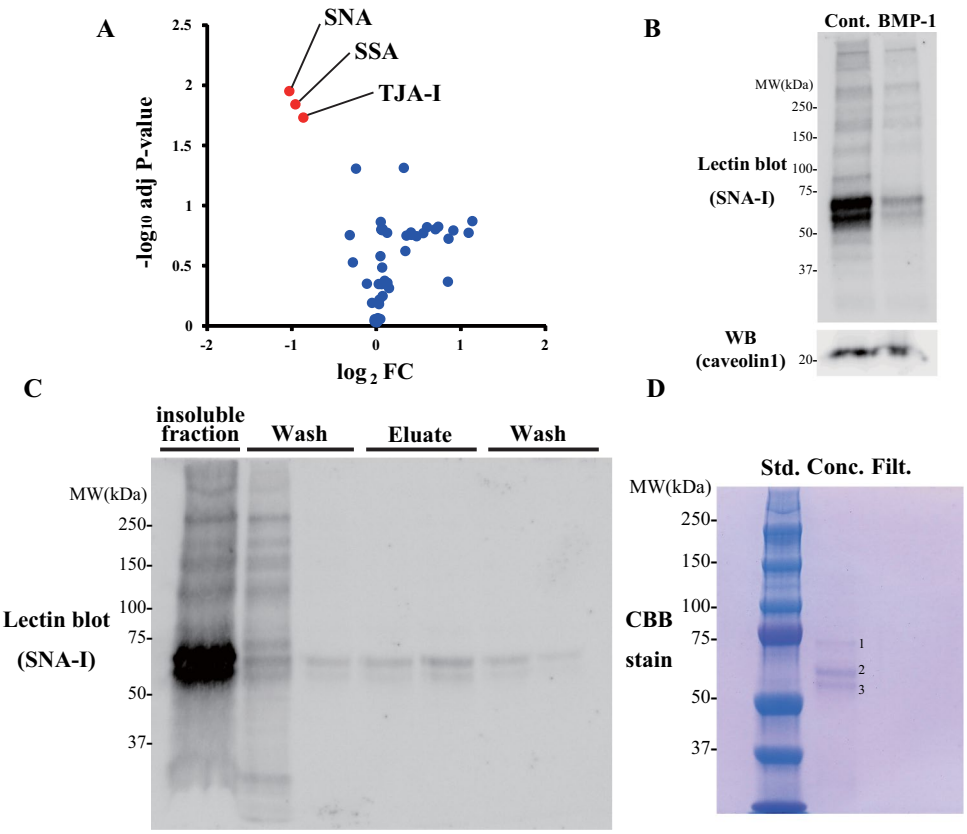

Fig. 1 A comprehensive analysis of BMP-1-altered glycosylation profiles in hDPCs. **A** The volcano plot represents fold change (x-axis) and *p*-values (y-axis) of signal intensities of each lectin between the absence or presence of rhBMP-1 (500 ng/mL) for 1 h. *Sambucus nigra* agglutinin (SNA), *Sambucus sieboldiana* agglutinin (SSA), and *Trichosanthes japonica* agglutinin-I (TJA-I), which commonly recognize α2,6-sia, showed significant reductions in signals. Results are from three different donors. Significant differences in lectin intensity were calculated by F-test. **B** A lectin-probed blotting analysis of the insoluble fraction (10 μg protein) from hDPCs. Nitrocellulose membranes were incubated with HRP-conjugated SNA followed by visualization. As expected, the signal of α2,6-sia was attenuated by BMP-1 compared to controls. **C** The enrichment of α2,6-sialylated glycoprotein from the insoluble fraction of hDPCs. After cell harvesting, the isolated insoluble fraction samples were suspended in adsorption buffer and applied to an SNA lectin column. After washing two times with adsorption buffer, SNA binding glycoproteins were eluted two times from the affinity column with elution buffer (sialyl-lactose). After elution, the column was washed again two times with adsorption buffer, and the purity of serial wash fractions and the eluate was assessed by SDS-PAGE with probing using HRP-conjugated SNA. **D** The eluate was desalted and concentrated by diafiltration. The concentrate (Conc.) and the filtrate (Filt.) were separated by SDS-PAGE and stained with CBB. Std. denotes protein molecular weight standards

(Fig. 2A). The GBA1 signal was increased in the presence of rhBMP-1 compared with that of the control. Based on this result, subsequent experiments focused on GBA1. To further investigate the subcellular localization of GBA1, we conducted immunofluorescence experiments using a confocal laser scanning microscope (Fig. 2B). In the control, GBA1 signals were detected in the nuclei of hDPCs but showed low immunofluorescence. In addition, these slight signals were distributed in the cytoplasm. Weak signals of GBA1 emanated from the nuclei at 5 min after the addition of rhBMP-1 to the cell culture. When the cells were treated with rhBMP-1 between 15 and 180 min, the signals of immunofluorescence were enhanced in a time-dependent manner and peaked at 60 min after stimulation. The quantification of the fluorescence intensity of nuclei demonstrating a GBA1 signal showed that the GBA1 in the nuclei was significantly increased in the presence of BMP-1 (Fig. 2C). Z-stack images of hDPCs showed that GBA1 signals were detected inside the nuclei as well as in the nuclear envelope (Fig. 2D). Since GBA1 is mostly considered a lysosomal enzyme, we further conducted a colocalization analysis of GBA1 and the lysosomal marker lysosome associated membrane protein 1 (LAMP1) (Fukuda 1991). LAMP1-positive compartments were scattered in the cytoplasm throughout the control and BMP-1 groups. Fluorescence signals of GBA1 were observed in the cytoplasm and colocalized with the LAMP1, but the signals were concomitantly increased in the nuclei upon BMP-1 administration (Fig. 2E). These results suggest that, contrary to expectation, BMP-1 induces GBA1 accumulation in the nucleus rather than the lysosome.

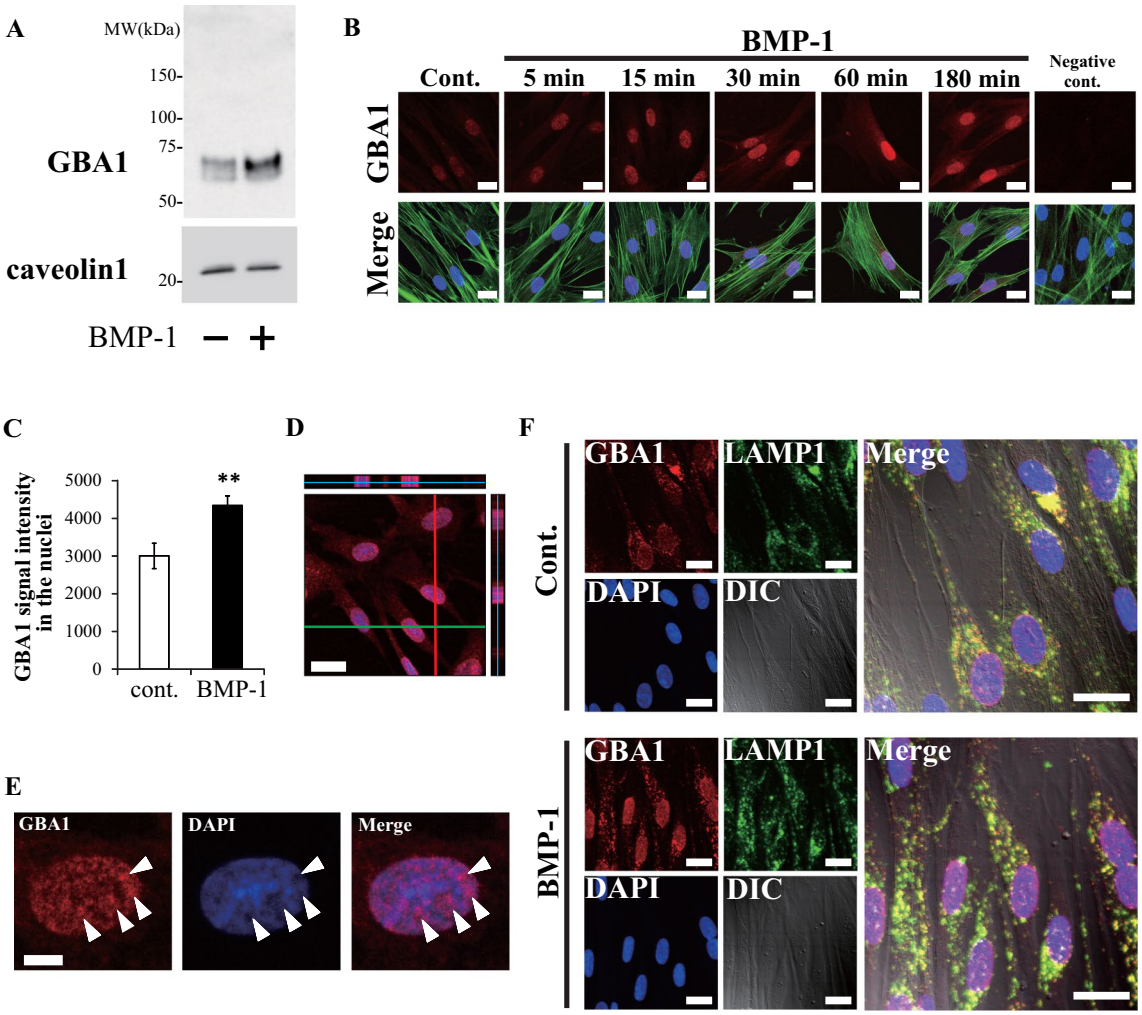

Fig. 2 BMP-1 regulates the nuclear accumulation of GBA1 in hDPCs. **A** To confirm the results of MS analysis, the insoluble fractions from hDPCs were analyzed by Western blotting with rabbit anti-GBA1 antibody. **B** BMP-1 facilitates the nuclear accumulation of GBA1. Cells were incubated with rhBMP-1 (500 ng/mL) for 5, 15, 30, 60, and 180 min. After fixation by paraformaldehyde, the signals of GBA1 were observed using a confocal laser scanning microscope. Pictures indicate GBA1 (Alexa fluor 594, red), filamentous actin (Alexa Fluor 488 phalloidin, green), and nuclei (DAPI, blue). Scale bars: 20 μm. Negative controls were treated without the primary antibody. **C** GBA1 signals were observed in three randomly chosen sites per three different experiments (n = 3). GBA1 signal intensity in the nuclei was quantified by measuring all of the nuclei in the pictures. Results are presented as the means ± SE. Statistical analysis was performed by Tukey's test. $^{**}P < 0.01$ versus control. **D** Orthogonal view from confocal z-stack images of hDPCs. hDPCs were incubated in the presence of rhBMP-1 (500 ng/mL) for 1 h. Pictures indicate GBA1 (Alexa fluor 594, red) and nuclei (DAPI, blue). Blue lines indicate the X/Y plane, the green line indicates the X/Z plane, and the red line indicates the Y/Z plane. **E** A typical image of GBA1 and nuclei from (**D**). GBA1 signals were observed in the low-density region of DAPI-staining (white arrowheads). (F) Cytoplasmic GBA1 is localized in lysosomes, and it also accumulates in the nucleus in the presence of BMP-1. hDPCs were incubated in the absence or presence of rhBMP-1 (500 ng/mL) for 1 h. After fixation by ice-cold methanol, the localization of GBA1 was observed using a confocal laser scanning microscope. Pictures indicate GBA1 (Alexa fluor 594, red), LAMP1 (Alexa Fluor 488, green), nuclei (DAPI, blue), and differential interference contrast (DIC) images. Scale bars: 20 μm

Contribution of GBA1 in BMP-1induced-CCN2 mRNA expression

We have previously reported that BMP-1 upregulates the expression of CCN2, which is well known as an osteogenesis/chondrogenesis marker, in hDPCs (Muromachi et al. 2015). To further investigate the function of GBA1 in hDPCs, we performed a GBA1 knockdown experiment using siRNA transfection. The protein expression of GBA1 was significantly reduced by the transfection with respective siRNAs, but not with a scramble siRNA as a control (Fig. 3A and B). Subsequently, real-time RT-PCR results showed that BMP-1-induced CCN2 mRNA expression was attenuated in the GBA1 siRNA-transfected cells compared with the scramble siRNA-transfected cells (Fig. 3C).

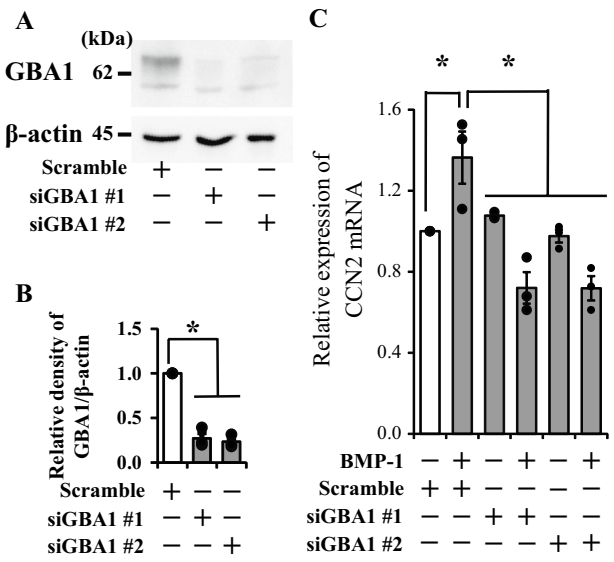

Fig. 3 Inhibition of BMP-1-induced CCN2 expression in hDPCs transfected with GBA1 siRNAs. **A** Protein levels of GBA1 and β-actin were detected by Western blotting in the cells transfected with GBA1 or scramble siRNAs. Cell lysates (5 μg protein) were used for immunoblotting. **B** Densitometric quantification of immunoreactive bands was calculated as the ratio of GBA1 to β-actin and is normalized against control. **C** BMP-1-induced CCN2 mRNA expression was attenuated in the cells transfected with siRNAs for GBA1 as compared to in scramble siRNA-transfected cells. Results are presented as the means ± SE. Statistical analysis was performed by Tukey's test. $^{*}P < 0.05$

Therefore, these data suggest that BMP-1 is a regulator of CCN2 through GBA1.

BMP-1-induced CCN2 expression dependently on importin-β-mediated nuclear import of GBA1

The results of immunofluorescence clearly indicated BMP-1 facilitates GBA1 nuclear accumulation. Given that BMP-1 regulates CCN2 expression via GBA1, it is plausible that the nuclear accumulation of GBA1 might correlate with the CCN2 expression. To address this possibility, we utilized importazole, a potent inhibitor of importin-β-mediated nuclear import (Soderholm et al. 2011). Immunofluorescence results showed that BMP-1-induced nuclear accumulation of GBA1 was suppressed by importazole (Fig. 4A). Additionally, we tested if nuclear export could regulate GBA1 nuclear accumulation caused by BMP-1 using KPT-276, a selective inhibitor of exportin 1 (*XPO1*) and its gene product chromosome maintenance region 1 (CRM1). As a result, nuclear accumulation of GBA1 was enhanced by KPT-276 even in the absence of BMP-1, whereas contrary to expectations, additional promotion of GBA1 nuclear accumulation in the presence of BMP-1 was not observed (Fig. 4A). Furthermore, we evaluated the effect of importazole on BMP-1-induced CCN2 mRNA expression. As expected, BMP-1-induced CCN2 mRNA expression was attenuated by importazole (Fig. 4B). These results suggest that the importin-β-mediated nuclear import of GBA1 contributes to BMP-1-induced CCN2 mRNA expression.

Discussion

In the present study, we showed that (i) BMP-1 attenuates the α2,6-sialylation of glycoproteins in the insoluble fraction of hDPCs, (ii) α2,6-sialylated glycoprotein can be identified by lectin-aided purification and an LC-MS/MS analysis, (iii) among the identified glycoproteins, the nuclear accumulation of GBA1 is promoted by BMP-1, and (iv) BMP-1-induced-CCN2 mRNA expression is attenuated in *GBA1*-silenced hDPCs, (v) importin-β-mediated nuclear import of GBA1 stimulates BMP-1-induced CCN2 mRNA expression (Fig. 5). These findings not only identified GBA1 as a targeting molecule of BMP-1 but also uncovered that BMP-1-GBA1 axis may have an epigenetic role in the transcriptional regulation of the *CCN2* gene.

Glycosylation is mostly known to occur in proteins located either at the cell membrane or in luminal compartments of specific subcellular organelles, while glyco-conjugation affects nuclear proteins. For instance, *O*-linked *N*-acetylglucosamine (O-GlcNAc) glycosylation of serine and threonine residues is a common post-translational modification of nuclear and cytosolic proteins (Hu et al. 2010). One specific example of glycoconjugation in the nucleus is the O-GlcNAcylation of histones (Sakabe et al. 2010). It is common knowledge that changes in oligosaccharide structures can regulate the stability and function of cellular glycoproteins. Notably, α2,6-sia modification has been implicated in numerous biologic processes through the modulation of protein subcellular localization and function (Cha et al. 2008; Kitazume et al. 2010; Amano et al. 2003). Through a lectin-aided evaluation, the present study revealed that BMP-1 dramatically attenuates the α2,6-sialylation of the insoluble fraction from hDPCs. The expression of α2,6-sia was estimated to be higher in undifferentiated cells than in differentiated cells (Tateno et al. 2011). Beneath severe dental caries, newly differentiated odontoblast-like cells from the subodontoblastic layer migrate to sites of injury following the loss of original odontoblasts (Sloan and Smith 2007). Thus, cellular glycome, especially α2,6-sialylation, might be a practical marker for evaluating the wound healing of the dentin-pulp complex. We also speculate that BMP-1 might be responsible for the differentiation of odontoblasts through glyco-alteration.

The MS analysis results of enriched glycoproteins suggest that α2,6-sialylation of GBA1 in hDPCs was reduced correspondingly upon the administration of BMP-1. GBA1,

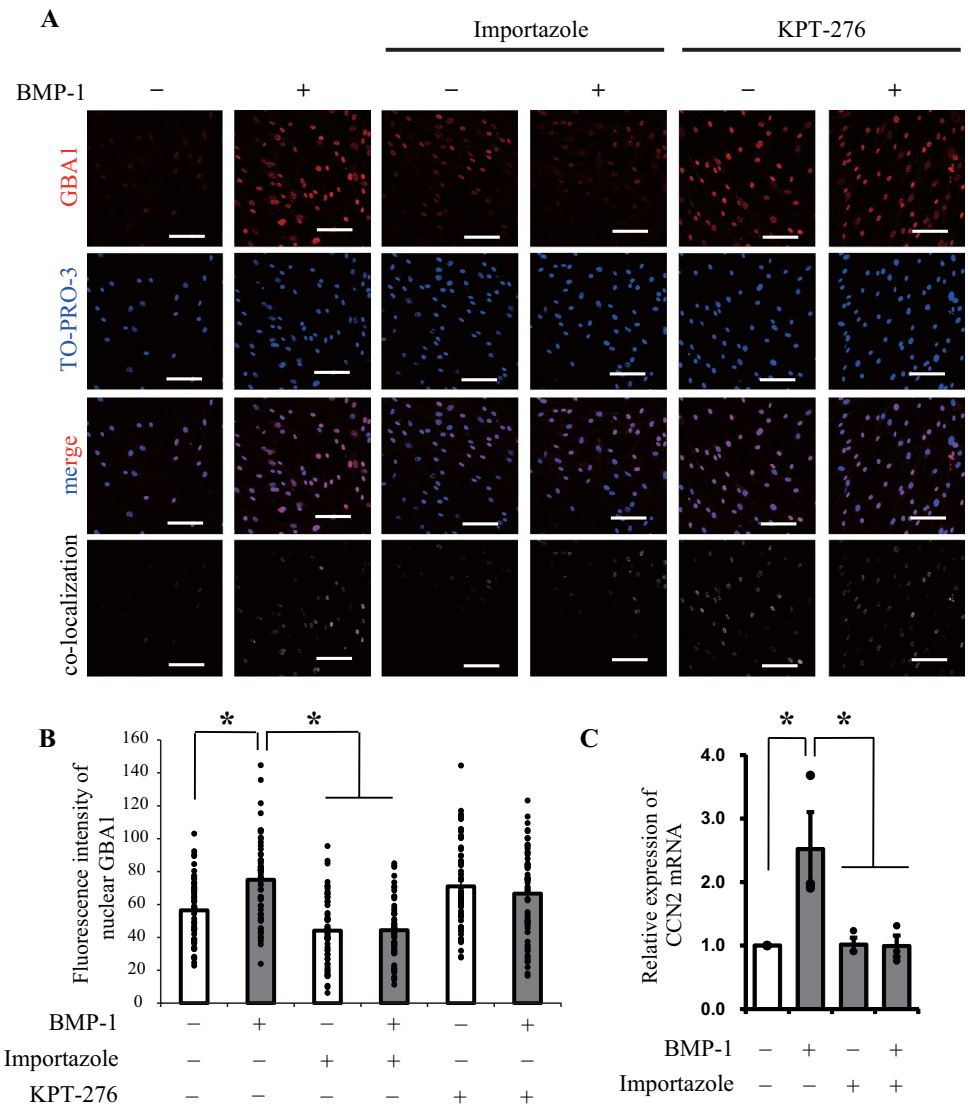

Fig. 4 Importin-β-mediated nuclear import of GBA1 stimulates BMP-1-induced CCN2 expression. **A** The cells were treated with BMP-1 (500 ng/mL) after the pretreatment of importazole (5 μM), KPT-276 (10 μM) for 1 h. Nuclear accumulation of GBA1 (red) was detected using a confocal laser scanning microscope. TO-PRO-3 iodide (blue) was used as a nuclear marker. Scale bars: 100 μm. **B** GBA1 signal intensity in the nuclei was quantified in randomly chosen sites per three different experiments (n = 60). **C** BMP-1-induced expression of CCN2 was attenuated in cells treated with importazole as compared to mRNA levels of CCN2 in control. Results are presented as the means ± SE. Statistical analysis was performed by Tukey's test. *$P < 0.05$

also called glucocerebrosidase, is an enzyme that hydrolyzes glucosylceramide (GlcCer) to glucose and ceramide (Ishibashi et al. 2013). In mammals, this hydrolase consists of three members: GBA1, non-lysosomal β-glucosylceramidase (GBA2), and cytosolic β-glucosidase (GBA3, also known as Klotho-related protein (KLrP)). Given that GBA1 is well-recognized as a lysosomal enzyme, we were interested in determining the subcellular localization of the enzyme. A colocalization study showed that cytoplasmic GBA1 is distributed in lysosomes and it also accumulates in the nucleus in the presence of BMP-1. This GBA1 subcellular localization is consistent with the findings of a previous report, which found that most GBA1 was detected in the microsomal and cytoplasmic fractions, although the nuclear fraction also showed some GBA1, based on an enzymatic activity assay (Sorge et al. 1987). These results together suggest a mechanism whereby GBA1 nuclear translocation can be regulated by BMP-1-induced α2,6-sia reduction through the lysosome-independent pathway. Furthermore, immunofluorescence results showed that GBA1 signals were located inside the nuclei and distributed in the low-density region of DAPI staining, which is recognized to indicate euchromatin (Saksouk et al. 2015). Chromatin can be categorized into two states of euchromatin and heterochromatin based on its degree of compaction (Ruthenburg et al. 2007). Heterochromatin is detectable by DAPI staining, and its signal intensity is six-fold higher than that of euchromatin (Bancaud et al. 2009). Euchromatin has been described as a transcriptionally active region usually characterized by unfolded conformation. With these studies in mind, it should be noted that GBA1 could be considered as a transcriptional regulator of genes. In fact in Fig. 3, the results of siRNA transfection experiments showed that BMP-1 failed to induce CCN2 mRNA expression in *GBA1*-null hDPCs. Furthermore, in Fig. 3C, GBA1 siRNA only affects BMP-1-induced CCN2 levels and not baseline. Such data suggests that GBA1

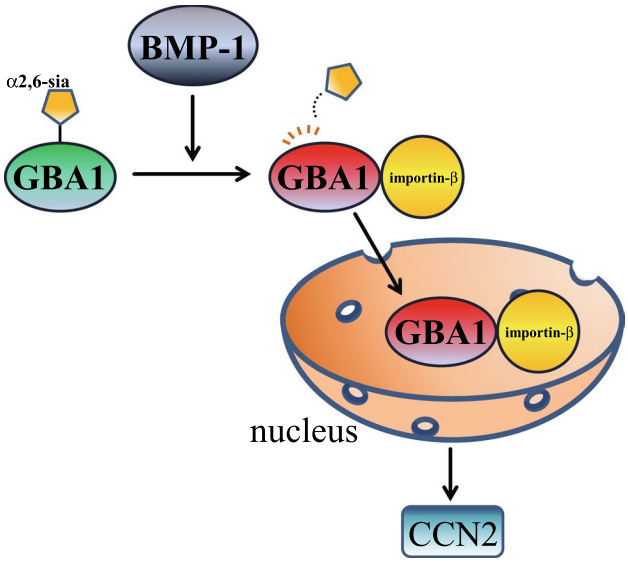

Fig. 5 Schematic representation of the mechanism of BMP-1-induced CCN2 expression. α2,6-sialylation of GBA1 is attenuated by BMP-1. Then, GBA1 translocates into the nucleus in a BMP-1-dependent manner. Finally, the BMP-1-induced GBA1 nuclear accumulation provokes CCN2 mRNA expression via importin-β mediated nuclear import pathway

may not involve in non-BMP-1 stimulated CCN2 mRNA expression.

Next, the mechanism by which GBA1 translocates into the nucleus was investigated. The experiments utilizing importazole showed that this small molecule inhibitor of nuclear import suppressed GBA1 nuclear accumulation. Importazole specifically inhibits the interaction between importin-β and Ran-GTP (Soderholm et al. 2011). The binding of Ran-GTP to importin-β causes a conformational change that results in the disassembly of the importin α/β-cargo complex (Lee et al. 2005), following cargo release into the nucleus. Therefore, the importin-β-Ran-GTP dependent nucleocytoplasmic pathway is associated with BMP-1-mediated GBA1 nuclear accumulation. Furthermore, Real-time PCR results showed that importazole attenuated BMP-1-induced CCN2 mRNA expression. Notably, we also found that CCN2 mRNA expression was significantly suppressed in *GBA1*-null hDPCs. Taken together, these results suggest that BMP-1-induced GBA1 nuclear accumulation provokes CCN2 mRNA expression via importin-β mediated nucleocytoplasmic pathway. Considering that BMP-1 attenuates α2,6-sia, these results led us to speculate that BMP-1 could act as a scaffolding protein mediating importin and the specific domain containing α2,6-sialylated N-glycan of GBA1 interaction, and following GBA1 nuclear translocation. The aspect of whether GBA1 is a directly binding regulatory protein of the *CCN2* gene remains an interesting project for future studies.

Mutations in the *GBA1* gene cause an impaired enzymatic function, inappropriate GBA1 localization, and decreased GBA1 stability (Beutler and Kuhl 1986; Liou et al. 2006; Schmitz et al. 2005). The appropriate subcellular localization of GBA1 affects its catalytic activity. Loss of GBA1 activity induces the accumulation of GlcCer in lysosomes, failing glycosphingolipid metabolism (Tybulewicz et al. 1992; Liu et al. 1998). Therefore, BMP-1 is considered essential for the maintenance of glycosphingolipid turnover through the modulation of GBA1. The importance of GlcCer degradation has been confirmed by the lethality of mice carrying *GBA* gene deletion (Tybulewicz et al. 1992; Liu et al. 1998). These knockout mice show reduced GBA1 activity and malformation of the epidermal permeability barrier compared with wild-type mice. The accumulation of GlcCer in lysosomes induced by GBA1 deficiency leads to Gaucher disease. Delayed tooth eruption has been reported in patients with Gaucher disease (Carter et al. 1998). Although further studies are needed, it is worth mentioning that the role of BMP-1 is not limited to the formation of bone and teeth; it might also be involved in Gaucher disease via the reduction of α2,6-sia from GBA1.

From a pathological point of view, CCN2 expression is increased in odontoblast-like cells beneath the caries lesion (Muromachi et al. 2015). In general, severe damage such as bacterial invasion promotes the migration of newly differentiated odontoblast-like cells to the injured sites leading to the formation of reparative dentin with a bone-like appearance (Bleicher 2014). The involvement of CCN2 in bone development is well documented (Takigawa 2013). Considering these findings with our present results, the BMP-1-GBA1-CCN2 axis is expected to be a candidate therapeutic target for dental pulp-preserving approaches.

Acknowledgements This study was supported by JSPS KAKENHI Grant-in-Aid for Scientific Research (C) #18K09587 and #21K09882. We express our sincere thanks to Dr. Masao YAMADA and GlycoTechnica, Ltd., for conducting the lectin microarray analysis and Shimadzu Techno-Research for conducting the LC-MS/MS analysis. We appreciate Dr. Fumihiko YOSHINO and Dr. Ayaka YOSHIDA for their helpful suggestions. MUROMACHI K expresses a special thanks to Tomomi, Kaho, Reika, and Charo MUROMACHI for their helpful support.

Data availability The mass spectrometry proteomics data have been deposited to the Figshare repository (https://figshare.com/) with the dataset identifier https://doi.org/10.6084/m9.figshare.15128802.

Declarations

Conflict of interest The authors declare no potential conflicts of interest with respect to the authorship and/or publication of this article.

References

Abbey SR, Eckhard U, Solis N, Marino G, Matthew I, Overall CM (2018) The human odontoblast cell layer and dental pulp

proteomes and N-terminomes. J Dent Res 97:338–346. https://doi.org/10.1177/0022034517736054

Amano M, Galvan M, He J, Baum LG (2003) The ST6Gal I sialyltransferase selectively modifies N-glycans on CD45 to negatively regulate galectin-1-induced CD45 clustering, phosphatase modulation, and T cell death. J Biol Chem 278:7469–7475. https://doi.org/10.1074/jbc.M209595200

Bancaud A, Huet S, Daigle N, Mozziconacci J, Beaudouin J, Ellenberg J (2009) Molecular crowding affects diffusion and binding of nuclear proteins in heterochromatin and reveals the fractal organization of chromatin. EMBO J 28:3785–3798. https://doi.org/10.1038/emboj.2009.340

Beutler E, Kuhl W (1986) Glucocerebrosidase processing in normal fibroblasts and in fibroblasts from patients with type I, type II, and type III gaucher disease. Proc Natl Acad Sci U S A 83:7472–7474. https://doi.org/10.1073/pnas.83.19.7472

Bleicher F (2014) Odontoblast physiology. Exp Cell Res 325:65–71. https://doi.org/10.1016/j.yexcr.2013.12.012

Bradford MM (1976) A rapid and sensitive method for the quantitation of microgram quantities of protein utilizing the principle of protein-dye binding. Anal Biochem 72:248–254. https://doi.org/10.1006/abio.1976.9999

Carter LC, Fischman SL, Mann J, Elstein D, Stabholz A, Zimran A (1998) The nature and extent of jaw involvement in Gaucher disease: observations in a series of 28 patients. Oral Surg Oral Med Oral Pathol Oral Radiol Endod 85:233–239. https://doi.org/10.1016/s1079-2104(98)90432-2

Cha SK, Ortega B, Kurosu H, Rosenblatt KP, Kuro-O M, Huang CL (2008) Removal of sialic acid involving Klotho causes cell-surface retention of TRPV5 channel via binding to galectin-1. Proc Natl Acad Sci U S A 105:9805–9810. https://doi.org/10.1073/pnas.0803223105

Fukuda M (1991) Lysosomal membrane glycoproteins. Structure, biosynthesis, and intracellular trafficking. J Biol Chem 266:21327–21330

Hu P, Shimoji S, Hart GW (2010) Site-specific interplay between O-GlcNAcylation and phosphorylation in cellular regulation. FEBS Lett 584:2526–2538. https://doi.org/10.1016/j.febslet.2010.04.044

Ishibashi Y, Kohyama-Koganeya A, Hirabayashi Y (2013) New insights on glucosylated lipids: metabolism and functions. Biochim Biophys Acta 1831:1475–1485. https://doi.org/10.1016/j.bbalip.2013.06.001

Kessler E, Takahara K, Biniaminov L, Brusel M, Greenspan DS (1996) Bone morphogenetic protein-1: the type I procollagen C-proteinase. Science 271:360–362. https://doi.org/10.1126/science.271.5247.360

Kitazume S, Imamaki R, Ogawa K, Komi Y, Futakawa S, Kojima S, Hashimoto Y, Marth JD, Paulson JC, Taniguchi N (2010) Alpha2,6-sialic acid on platelet endothelial cell adhesion molecule (PECAM) regulates its homophilic interactions and downstream antiapoptotic signaling. J Biol Chem 285:6515–6521. https://doi.org/10.1074/jbc.M109.073106

Lee SJ, Matsuura Y, Liu SM, Stewart M (2005) Structural basis for nuclear import complex dissociation by RanGTP. Nature 435:693–696. https://doi.org/10.1038/nature03578

Li SW, Sieron AL, Fertala A, Hojima Y, Arnold WV, Prockop DJ (1996) The C-proteinase that processes procollagens to fibrillar collagens is identical to the protein previously identified as bone morphogenic protein-1. Proc Natl Acad Sci U S A 93:5127–5130. https://doi.org/10.1073/pnas.93.10.5127

Liou B, Kazimierczuk A, Zhang M, Scott CR, Hegde RS, Grabowski GA (2006) Analyses of variant acid beta-glucosidases: effects of Gaucher disease mutations. J Biol Chem 281:4242–4253. https://doi.org/10.1074/jbc.M511110200

Liu Y, Suzuki K, Reed JD, Grinberg A, Westphal H, Hoffmann A, Döring T, Sandhoff K, Proia RL (1998) Mice with type 2 and 3 gaucher disease point mutations generated by a single insertion mutagenesis procedure. Proc Natl Acad Sci U S A 95:2503–2508. https://doi.org/10.1073/pnas.95.5.2503

Muromachi K, Kamio N, Matsuki-Fukushima M, Nishimura H, Tani-Ishii N, Sugiya H, Matsushima K (2015) CCN2/CTGF expression via cellular uptake of BMP-1 is associated with reparative dentinogenesis. Oral Dis 21:778–784. https://doi.org/10.1111/odi.12347

Ruthenburg AJ, Li H, Patel DJ, Allis CD (2007) Multivalent engagement of chromatin modifications by linked binding modules. Nat Rev Mol Cell Biol 8:983–994. https://doi.org/10.1038/nrm2298

Sakabe K, Wang Z, Hart GW (2010) Beta-N-acetylglucosamine (O-GlcNAc) is part of the histone code. Proc Natl Acad Sci U S A 107:19915–19920. https://doi.org/10.1073/pnas.1009023107

Saksouk N, Simboeck E, Déjardin J (2015) Constitutive heterochromatin formation and transcription in mammals. Epigenetics Chromatin 8:3. https://doi.org/10.1186/1756-8935-8-3

Schmitz M, Alfalah M, Aerts JM, Naim HY, Zimmer KP (2005) Impaired trafficking of mutants of lysosomal glucocerebrosidase in Gaucher's disease. Int J Biochem Cell Biol 37:2310–2320. https://doi.org/10.1016/j.biocel.2005.05.008

Sloan AJ, Smith AJ (2007) Stem cells and the dental pulp: potential roles in dentine regeneration and repair. Oral Dis 13:151–157. https://doi.org/10.1111/j.1601-0825.2006.01346.x

Soderholm JF, Bird SL, Kalab P, Sampathkumar Y, Hasegawa K, Uehara-Bingen M, Weis K, Heald R (2011) Importazole, a small molecule inhibitor of the transport receptor importin-β. ACS Chem Biol 6:700–708. https://doi.org/10.1021/cb2000296

Sorge JA, West C, Kuhl W, Treger L, Beutler E (1987) The human glucocerebrosidase gene has two functional ATG initiator codons. Am J Hum Genet 41:1016–1024

Steiglitz BM, Ayala M, Narayanan K, George A, Greenspan DS (2004) Bone morphogenetic protein-1/Tolloid-like proteinases process dentin matrix protein-1. J Biol Chem 279:980–986. https://doi.org/10.1074/jbc.M310179200

Syx D, Guillemyn B, Symoens S, Sousa AB, Medeira A, Whiteford M, Hermanns-Lê T, Coucke PJ, De Paepe A, Malfait F (2015) Defective proteolytic processing of fibrillar procollagens and prodecorin due to biallelic BMP1 mutations results in a severe, progressive form of osteogenesis imperfecta. J Bone Miner Res 30:1445–1456. https://doi.org/10.1002/jbmr.2473

Takahara K, Lyons GE, Greenspan DS (1994) Bone morphogenetic protein-1 and a mammalian tolloid homologue (mTld) are encoded by alternatively spliced transcripts which are differentially expressed in some tissues. J Biol Chem 269:32572–32578

Takigawa M (2013) CCN2: a master regulator of the genesis of bone and cartilage. J Cell Commun Signal 7:191–201. https://doi.org/10.1007/s12079-013-0204-8

Tateno H, Toyota M, Saito S, Onuma Y, Ito Y, Hiemori K, Fukumura M, Matsushima A, Nakanishi M, Ohnuma K, Akutsu H, Umezawa A, Horimoto K, Hirabayashi J, Asashima M (2011) Glycome diagnosis of human induced pluripotent stem cells using lectin microarray. J Biol Chem 286:20345–20353. https://doi.org/10.1074/jbc.M111.231274

Tsuchiya S, Simmer JP, Hu JC, Richardson AS, Yamakoshi F, Yamakoshi Y (2011) Astacin proteases cleave dentin sialophosphoprotein (dspp) to generate dentin phosphoprotein (dpp). J Bone Miner Res 26:220–228. https://doi.org/10.1002/jbmr.202

Tybulewicz VL, Tremblay ML, LaMarca ME, Willemsen R, Stubblefield BK, Winfield S, Zablocka B, Sidransky E, Martin BM, Huang SP (1992) Animal model of Gaucher's disease from targeted disruption of the mouse glucocerebrosidase gene. Nature 357:407–410. https://doi.org/10.1038/357407a0

Urist MR, Iwata H, Ceccotti PL, Dorfman RL, Boyd SD, McDowell RM, Chien C (1973) Bone morphogenesis in implants of insoluble bone gelatin. Proc Natl Acad Sci U S A 70:3511–3515. https://doi.org/10.1073/pnas.70.12.3511

Varki A (1993) Biological roles of oligosaccharides: all of the theories are correct. Glycobiology 3:97–130. https://doi.org/10.1093/glycob/3.2.97

von Marschall Z, Fisher LW (2010) Dentin sialophosphoprotein (DSPP) is cleaved into its two natural dentin matrix products by three isoforms of bone morphogenetic protein-1 (BMP1). Matrix Biol 29:295–303. https://doi.org/10.1016/j.matbio.2010.01.002

Wang J, Muir AM, Ren Y, Massoudi D, Greenspan DS, Feng JQ (2017) Essential roles of bone morphogenetic protein-1 and mammalian tolloid-like 1 in postnatal root dentin formation. J Endod 43:109–115. https://doi.org/10.1016/j.joen.2016.09.007

Wozney JM, Rosen V, Celeste AJ, Mitsock LM, Whitters MJ, Kriz RW, Hewick RM, Wang EA (1988) Novel regulators of bone formation: molecular clones and activities. Science 242:1528–1534. https://doi.org/10.1126/science.3201241